Material testing method for understanding rubber's mechanical characteristics
Quasi-Static Tension Test

1 Introduction

In this working group, we conduct tension tests of rubber materials to characterize their history curves obtained from biaxial tension tests. Three different kinds of tests, uniaxial tension test, equi-biaxial tension test, and strip-biaxial tension test are carried out. We correct the measured displacement values by using strain fields measured from the specimen's photographic images in order to obtain the actual strain data. In this report, we firstly outline the equipment for biaxial tension tests. Secondly, we present the shapes or other characteristics of the specimens used in uniaixial tension tests, equi-biaxial tension tests and strip-biaxial tension tests. Finally, actual test procedures are explained.

2 Experimental equipment.

In this working group in JANCAE, we conduct material tests to characterize the history curves of rubber materials. A testing device for biaxial tension tests is used to elongate a specimen for three cycles. The deformation rate is controlled by an outside device. In this working group, trains calculated from measured displacements are corrected by an image processing. Images are taken by a digital CCD camera placed on the top of the biaxial tension device, and at the same time the load and displacement are measured. Fig. 1 shows the schematic of the biaxial tension device.

Since very low current flew out of a PC used for controlling the devices, electric noise occurred. Therefore, we blocked the noise by using an outlet with three lines, one of which is connected to the ground. Below, we show the outline of individual experimental equipments.

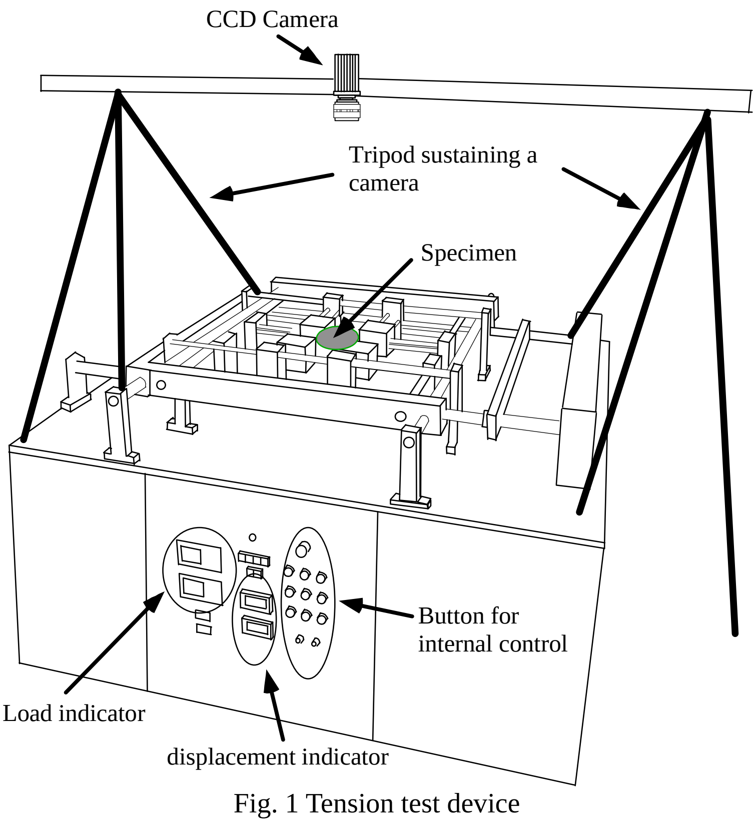

Fig. 1 Tension test device

2.1 Biaxial tension test

The biaxial tension test device used for this experiment moves its two arms along the center lines of a specimen to apply strains on it. The performances of the device are presented in table 1. The biaxial tension device and the specimen are shown below.

Figure 2 is an entire view of the biaxial tensile test device. Here, the *X*- and *Y*-directions are defined as illustrated in the figure.

The specimen is set so as to be pinched by chucks. Different chucks are used for specimens in tension and biaxial tests, which are shown in Figs.3 and 4, respectively.

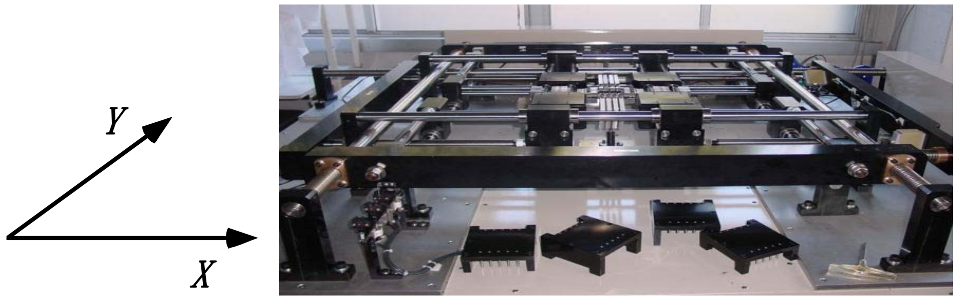

Fig. 2 Entire view of the biaxial tension test device

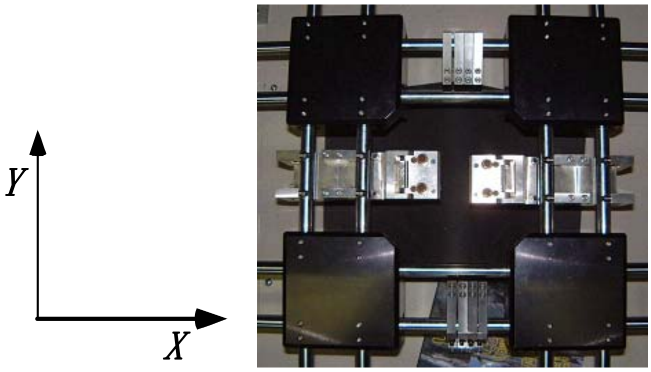

Fig. 3 Chuck of the uniaxial tension test device

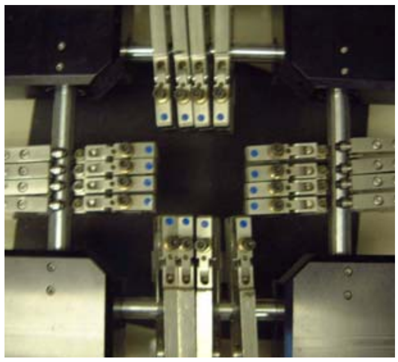

Fig. 4 Chuck for the biaxial tension test device

Table 1 Performance of the biaxial tension device

	Usage (Control and performance)
X-Y axis driving	Motor: HC－KFS43G2 1/20, 2 units
Speed setting	Independent (Internal control) vernier dial and digital display
Elongation speed	100 – 1200 mm/min (1.6 to 20 mm/sec)
Displacement display	Distance detection by potentionmeter. Format: LP－200F MIDORI PRECISIONS CO., LTD.
Distance display	Digital display: from 0 (Size within chuck: 50) to 999mm
Device elongation range	X-axis: from 50 to 400 mm, Y-axis: from 50 to 280 mm
Basic elongation range	X-axis: from 60 to 360 mm, Y-axis: from 60 to 240 mm
	DC 0 – 10v with analog output 1.0 V (X-axis: scale 40 mm) 1.0 V (Y-axis scale 35.82 mm)
Detection by load controlling load cell	Load cell TU-BR 500N (51.02 kg), two units each
	Amplifier TD-320A, TEAC Corporation
	Output by an open collector with upper limit: DC 0 to 10V with analog output
	10.0 V at 999.9 N, implying 100 N/1.0 V
Speed instruction by external control	Analog input: DC0 – 10.0 V (20mm/sec)
Power source	AC200 - 220V 15 - 20A (Current requirement less than 6A)
	During operation as interlocked, operation stops when top/bottom/corners are outputted for a load cell protection. Internal/external overrun sensor is arranged for the width drawn due to incorrect instruction.

2.2 Image capturing equipment

Figure 5 shows the digital CCD camera used in the image capturing to obtain displacement data. The performance of this camera is presented in Table 2. Since the spatial resolution is set at 2048×2000 [pixels] in this test, the temporal resolution is expressed in the formula given below. Table 1 indicates a temporal resolution in the case of spatial resolution of 2048 ×2048 [pixels].

Assume that it takes t [sec/frame] to record one image frame,

$$t = (11.4 + 0.0242y) \times 10^{-3} \tag{1}$$

where y [pixel] is the spatial resolution in the vertical direction. Therefore, assuming the temporal resolution is f [frame/sec], we have

$$f = \frac{1}{t} \tag{2}$$

which means the temporal resolution is $f \fallingdotseq 16.40$.

Fig. 5 Digital CCD Camera

Table 2 Performance of digital CCD camera

Name	Adimec-4000m
Spatial resolution [pixel]	2048×2048
Temporal resolution [frame/sec]	16.4
Recording method	Progressive scan
Image file format	8bit grayscale

3 Outline of specimens

3.1 Shape and dimensions of specimen for uniaxial tension test

Figure 6 present the shape and dimensions of a specimen, and Figure 7 shows the photo of an actual specimen for uniaxial tension tests. A uniaxial tension test in this context indicates a loading scheme in which a specimen is elongated only in one direction and the deformation in the direction perpendicular to the tensile direction is not constrained. Figure 8 shows an appearance of actual testing. We made a specimen for a uniaxial tension test by dividing a specimen for a biaxial tension test into two and by cutting out the chuck portions arranged in the direction perpendicular to the tensile direction. The maximum stroke of the chuck for a uiaxial tension test is 360 [mm] and is attached along the X-axis.

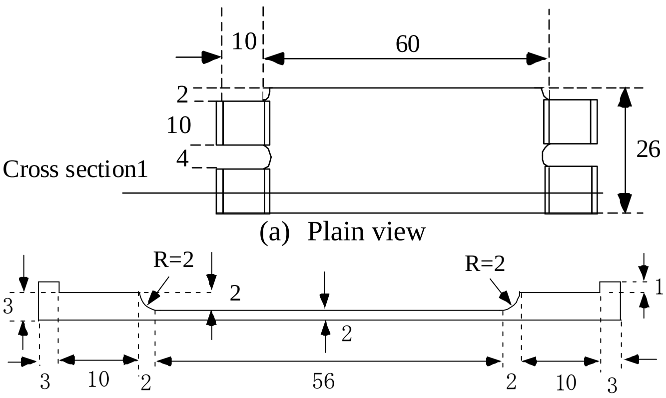

(a) Plain view

(b) Cross section view along the cross section 1

Fig. 6 Shape and dimensions of a specimen for a uniaxial tension test

Fig. 7 Photo of a specimen for a uniaxial tension test

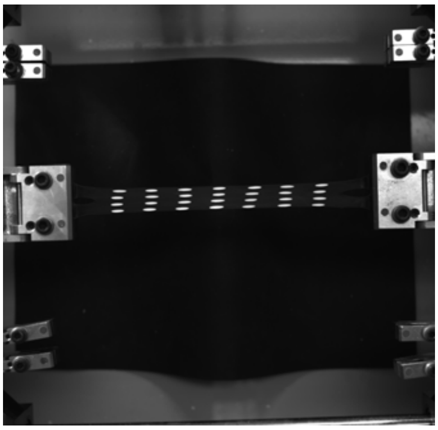

Fig. 8 Appearance of a uniaxial tension test

3.2 Shape of specimen for biaxial tensile test

Figure 9 shows the shape and dimensions of a specimen, and Figure 10 is a photo of a actual specimen. The biaxial tension test device can impose arbitrary deformations on a specimen in the two direction independently (referred to as X-axis and Y-axis). This specimen is used for biaxial tension tests. In a strip-biaxial tension test, a specimen is deformed in the X-direction, and the stretch in the Y-direction is fixed. In a equi-biaxial test, a specimen is elongated in both X- and Y-directions at the same loading speed and amplitude. Figures 11 and 12 show the appearances of these tests.

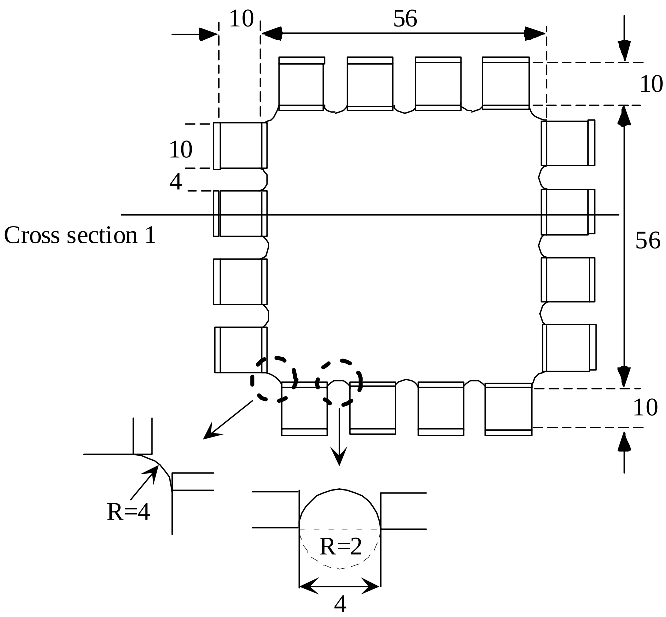

(a) Plain view

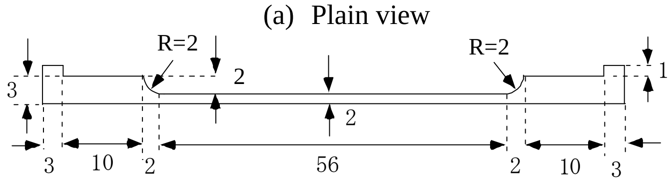

(b) Cross section view along the cross section 1

Fig. 9 Shape of specimen for biaxial tests

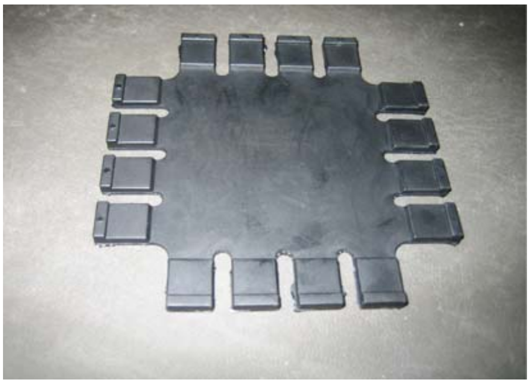

Fig. 10 Photo of a specimen for biaxial tension tests

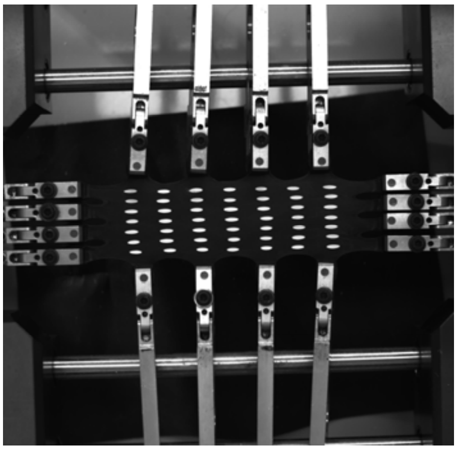

Fig. 10 Appearance of a strip-biaxial tension test

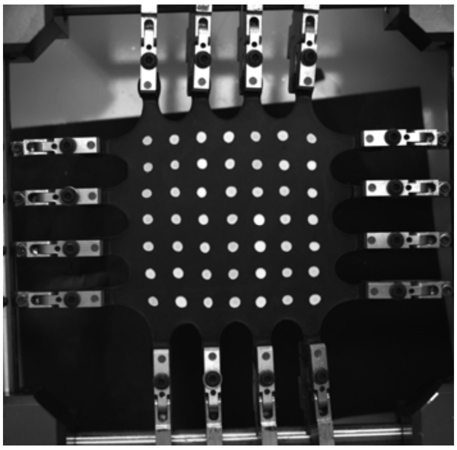

Fig. 11 Appearance of a equi-biaxial tension test

3.3 Types of rubber

Each rubber has its own hardness and damping characteristics. The damping values of a rubber with hardness 50 are tanδ=0.03 and tanδ=0.05, while those with hardness 65 are tanδ=0.20 and tanδ=0.27. The names of these materials are defined as in Table 3. Also, tanδ is called the loss coefficient, which indicates the damping performance (internal friction) of a rubber.

Table 3 Names of rubbers

Namel	Material A	Material B	Material C	Material D
Hardness	50	65	50	65
Damping	tanδ=0.03	tanδ=0.05	tanδ=0.20	tanδ=0.27

4 Testing method

4.1 Testing procedure

As described in the beginning of this report, the picture images of the deformation process of a specimen are captured by a CCD camera placed on the top of the test device and the strain values measured are corrected with the obtained image information (details are omitted here).

Time intervals for capturing picture images are changed according to tension speed and amplitude. The number of recorded images is 100 pictures per half amplitude motion for a specimen, so about 200 pictures are captured in a single test.

Table 4 indicates the number of specimens used in each test. The uniaxial tension tests were conducted three times at each of the loading speed of 2 m/sec and 20 mm/sec. The strip-biaxial tension tests were conducted once at each of the loading speed of 2 m/sec and 20mm/sec. The equi-biaxial tests were conducted once at each of the loading speed of 0.6 mm/sec, 2m/sec and 20mm/sec. For image capturing, an additional test was conducted for each material, each speed and each loading speed.

Table 4 Number of specimens (Unit: piece)

Uniaxial	Strip-biaxia	Equi-biaxial
28	16	24

4.2 biaxial tension tests

In this working group, we conducted three different kinds of tension tests as follows:

(1) Uniaxial tension test
(2) Strip-biaxial tension test
(3) Equi-biaxial tension test

Using the results of these three tests, we will characterize the energy of rubber for each test.

Uniaxial tension tests were conducted with a specimen shown in Fig. 7. At the same time, in a test accompanying image capturing to correct measured strain values, we used a specimen with white dots being drawn as shown in Fig. 13 and captured its deformation by a CCD camera to measure their displacements.

The strip-biaxial and equi-biaxial tension tests were conducted with a specimen shown in Fig. 10. Like in the uniaxial tests, in a test accompanying image capturing, we used a specimen with white dots being drawn as shown in Fig. 14 and captured its deformation by a CCD camera to measure their displacements.

Those tests were conducted at the elongation speed of 2 [mm/sec] and 20 [mm/sec] to study the effects of energy absorption in response to the change of the loading speed. Since the test results showed a similar trend irrespective of loading methods, we additionally conducted only for a equi-biaxial test at the loading speed of 0.6 [mm/sec]. The initial value and increment of the loading amplitude for one of the three uniaxial tension tests are 1.5 and 0.25, respectively, while those of the other two are 1.5 and 0.5, respectively. The tests were continued until a specimen is broken. On the other hand, the initial value and increment of the loading amplitude the strip-biaxial and equi-biaxial tension tests are 1.5 and 0.25, respectively, and the tests were continued until a specimen is broken. Also, an image capturing at every test was conducted for the amplitude smaller than the stretch value at fracture by one. Sampling frequencies were 2Hz, 5Hz and 50Hz for 0.6 [mm/sec], 2 [mm/sec] and 20 [mm/sec], respectively. Temperatures were maintained within the range of about 18 to 22°C in all the tests. Table 5 indicates a list of conducted tests and Table 6 indicates a list of sampling frequencies at each loading speed.

Fig. 13 Uniaxial test's specimen for image capturing

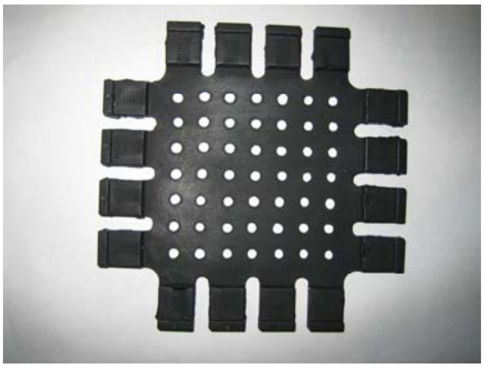

Fig. 14 Biaxial tests' specimen for image capturing

Table .5 Loading conditions of the tests

Name of Specimen	Loading method	Temp. (°C)	Humidity (%)	Loading Speed(mm/sec)	Amplitude (mm)
	Equi-biaxial	20	37		90, 105, 120, 135, 150, 165
	Strip-biaxial	20	37		90, 105, 120, 135, 150, 165
	Uniaxial	20	23	20mm/sec	90, 120, 150, 180, 210, 240
	Equi-biaxial	20	43		90, 105, 120, 135, 150, 165, 180
	Strip-biaxial	20	41		90, 105, 120, 135, 150, 165, 180, 195
		20	36		90, 105, 120, 135, 150, 165, 180, 195, 210, 225, 240
		20	36		90, 120, 150, 180, 210, 240
	Uniaxial	20	36	2mm/sec	90, 120, 150, 180, 210, 240
A	Equi-biaxial	20	36	0.6mm/sec	90, 105, 120, 135, 150, 165, 180
	Equi-biaxial	19	41		90, 105, 120, 135, 150
	Strip-biaxial	20	26		90, 105, 120, 135, 150, 165, 180, 195
	Uniaxial	20	23	20mm/sec	90, 120, 150, 180
	Equi-biaxial	17	44		90, 105, 120, 135, 150, 165
	Strip-biaxial	18	42		90, 105, 120, 135, 150, 165, 180, 195, 210
		20	33		90, 105, 120, 135, 150, 165, 180, 195, 210, 225
		20	33		90, 120, 150, 180, 210
	Uniaxial	20	33	2mm/sec	90, 120, 150, 180
B	Equi-biaxial	20	36	0.6mm/sec	90, 105, 120, 135, 150, 165, 180
	Equi-biaxial	18	42		90, 105, 120, 135, 150, 165
	Strip-biaxial	18	42		90, 105, 120, 135, 150, 165, 180, 195, 210, 225, 240, 255, 270, 285, 300
		22	33		90, 105, 120, 135, 150, 165, 180, 195, 210, 225, 240, 255, 270, 285, 300
		21	35		90, 120, 150, 180, 210, 240, 270, 300
	Uniaxial	20	35	20mm/sec	90, 120, 150, 180, 210, 240, 270, 300
	Equi-biaxial	20	41		90, 105, 120, 135, 150, 165, 180, 195
	Strip-biaxial	20	35		90, 105, 120, 135, 150, 165, 180, 195, 210
		19	50		90, 105, 120, 135, 150, 165, 180, 195, 210, 225, 240, 255, 270, 285, 300
		19	50		90, 120, 150, 180, 210, 240, 270, 300
	Uniaxial	19	50	2mm/sec	90, 120, 150, 180, 210, 240, 270, 300
C	Equi-biaxial	20	44	0.6mm/sec	90, 105, 120, 135, 150
	Equi-biaxial	19	55		90, 105, 120, 135, 150, 165, 180, 195
	Strip-biaxial	20	50		90, 105, 120, 135, 150, 165, 180, 195, 210, 225
		19	51		90, 120, 150, 180, 210, 240, 270
		19	51		90, 120, 150, 180, 210, 240, 270, 300
	Uniaxial	19	51	20mm/sec	90, 120, 150, 180, 210, 240, 270, 300
	Equi-biaxial	20	51		90, 105, 120, 135, 150, 165, 180
	Strip-biaxial	20	51		90, 105, 120, 135, 150, 165, 180, 195, 210, 225
		19	54		90, 105, 120, 135, 150, 165, 180, 195, 210, 225, 240, 255, 270
		19	54		90, 120, 150, 180, 210, 240, 270, 300
	Uniaxial	19	54	2mm/sec	90, 120, 150, 180, 210, 240, 270, 300
D	Equi-biaxial	21	26	0.6mm/sec	90, 105, 120, 135, 150, 165, 180

Table 6 Sampling frequency at each loading speed (Unit: Hz)

Loading speed	0.6 mm/sec	2 mm/sec	20 mm/sec
Sampling frequency	2	5	50

5 Treating method of experimental results

5.1 How to calculate strain field

By using the coordinate data at each point in a specimen obtained by an image processing (details are omitted here), we follow the displacements at the center of a white dot marked on the specimen, and calculate strains by comparing the images before and after the deformation.

The center point of a square consisting of four coordinate data points in a specimen is defined as one node of a four-node element. Strains in the element were calculated by interpolation with appropriate interpolation functions.

(1) Calculation of strain field

(a) Interpolation of displacement

A displacement value known at *k*th point (hereinafter referred to as node *k*) by the image processing is denoted by $u_i^{(k)}$, and the position of a dot in the undeformed state is denoted by $X_i^{(k)}$. Then, the displacement is interpolated according to the following formula:

$$u_1 = \sum_{k=1}^{n} N^{(k)} u_1^{(k)} = \{N\}^T \{u_1\} \quad (3a)$$

$$u_2 = \sum_{k=1}^{n} N^{(k)} u_2^{(k)} = \{N\}^T \{u_2\} \quad (3b)$$

where *i*=1 indicates the *X*-axis and *i*=2 the *Y*-axis. Here, $u_i^{(k)}$ is a value of the displacement u_i at node *k*, and $N^{(k)}$ is an interpolation function associated with $u_1^{(k)}$ and $u_2^{(k)}$. Each vector in formulae (3a) and (3b) are defined as follows;

$$\{u_1\}^T = \{u_1^{(1)}, u_1^{(2)}, \cdots\cdots, u_1^{(n)}\} \quad (4a)$$

$$\{u_2\}^T = \{u_2^{(1)}, u_2^{(2)}, \cdots\cdots, u_2^{(n)}\} \quad (4b)$$

$$\{N\}^T = \{N^{(1)}, N^{(2)}, \cdots\cdots, N^{(n)}\} \quad (4c)$$

where *n* indicates the number of nodal points of elements being used. When a square consisting four points are used as one element of an interpolation function in the above formulae, we have *n*=4 and a specific interpolation function associated with each nodal point is expressed as follows;

$$N^{(1)} = \frac{1}{4}(1-\xi)(1-\eta) \quad (5a)$$

$$N^{(2)} = \frac{1}{4}(1+\xi)(1-\eta) \quad (5b)$$

$$N^{(3)} = \frac{1}{4}(1+\xi)(1+\eta) \quad (5c)$$

$$N^{(4)} = \frac{1}{4}(1-\xi)(1+\eta) \quad (5d)$$

In the above formula, ξ and η are within $-1 \le \xi, \eta \le 1$, which are called the natural coordinates (Fig. 15) by finite element method. In this working group, the center of a square consisting four points are used, we used $\xi = \eta = 0$. These are regarded as a kind of parameters and have the following relations with spatial variables (X_1, X_2):

$$X_1 = N^{(k)} X_1^{(k)} \quad (6b)$$

$$X_2 = N^{(k)} X_2^{(k)} \quad (6b)$$

where $(X_1^{(k)}, X_2^{(k)})$ are a specific numerical values of (X_1, X_2) at a node *k*.

With these interpolation functions, we treated the experimental results. The target of the interpolation is a deformation gradient tensor.

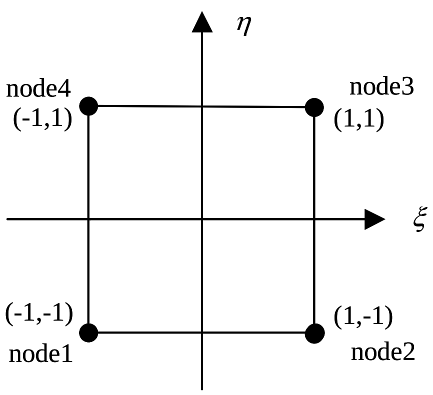

Fig. 15 Natural coordinate system

(b) Calculation of the deformation gradient tensor

Denoting the position of a material point in the reference configuration (undeformed state) by X_i and the current position (after deformation) by x_i, the deformation gradient tensor is defined as

$$F_{ij} = \frac{\partial x_i}{\partial X_i} \tag{7}$$

where the current position x_i is

$$x_i = u_i + X_i \tag{8}$$

Thus, when substituted to formula (10), this can be written as

$$F_{ij} = \frac{\partial (u_i + X_i)}{\partial X_j} = \delta_{ij} + \frac{\partial u_i}{\partial X_j} \tag{9}$$

Substitution of this expression into (6) yields

$$F_{ij} = \delta_{ij} + \frac{\partial \{N\}^T \{u_i\}}{\partial X_j} = \delta_{ij} + \frac{\partial \{N\}^T}{\partial X_j}\{u_i\} \tag{10}$$

From this, if each component of

$$\frac{\partial \{N\}^T}{\partial X_j} = \left\{ \frac{\partial N^{(1)}}{\partial X_j}, \frac{\partial N^{(2)}}{\partial X_j} \cdots \frac{\partial N^{(n)}}{\partial X_j} \right\}^T \tag{11}$$

can be calculated, the deformation gradient tensor component F_{ij} can be obtained. For the details of how to calculate formula (14) is explained in (3) later.

(c) Calculation of the right Cauchy-Green deformation tensor and Green_Lagrange strain

According to the definition, the right Cauchy-Green deformation tensor is calculated by the formula

$$\boldsymbol{C} = \boldsymbol{F}^T \cdot \boldsymbol{F} \tag{12}$$

and the Green_Lagrange strain is defined as

$$\boldsymbol{E} = \frac{1}{2}(\boldsymbol{C} - \boldsymbol{I}) \tag{13}$$

where, $\boldsymbol{I}$ is a unit matrix. When each component of the deformation gradient tensor $\boldsymbol{F}$ is calculated from the formula (13), the components of the above two tensors can be easily obtained.

(2) Spatial derived function of interpolation function

As indicated by the formula (13), to obtain the specific values of strain and etc., one have to evaluate derivatives of interpolation function $N^{(k)}$ with respect to X_1 or X_2. However, the interpolation function is directly a function of parameter (ξ, η) and directly associated with (X_1, X_2) by the formula (9). Accordingly, when the chain rule of differentiation is applied in a general manner, we have

$$\frac{\partial N^{(k)}}{\partial X_1} = \frac{\partial N^{(k)}}{\partial \xi} \cdot \frac{\partial \xi}{\partial X_1} + \frac{\partial N^{(k)}}{\partial \eta} \cdot \frac{\partial \eta}{\partial X_1} \tag{14a}$$

$$\frac{\partial N^{(k)}}{\partial X_2} = \frac{\partial N^{(k)}}{\partial \xi} \cdot \frac{\partial \xi}{\partial X_2} + \frac{\partial N^{(k)}}{\partial \eta} \cdot \frac{\partial \eta}{\partial X_2} \tag{14b}$$

When the above formulas are summarized and described in a matrix, we have

$$\begin{Bmatrix} \dfrac{\partial N^{(k)}}{\partial X_1} \\ \dfrac{\partial N^{(k)}}{\partial X_2} \end{Bmatrix} = \begin{bmatrix} \dfrac{\partial \xi}{\partial X_1} & \dfrac{\partial \eta}{\partial X_1} \\ \dfrac{\partial \xi}{\partial X_2} & \dfrac{\partial \eta}{\partial X_2} \end{bmatrix} \begin{Bmatrix} \dfrac{\partial N^{(k)}}{\partial \xi} \\ \dfrac{\partial N^{(k)}}{\partial \eta} \end{Bmatrix} \tag{15}$$

in which

$$\left\{ \frac{\partial N^{(k)}}{\partial \xi} \frac{\partial N^{(k)}}{\partial \eta} \right\}^T \tag{16}$$

can easily be calculated from formula (5). On the other hand, the right side matrix of formula (15) is calculated as explained below. Firstly, assuming that interpolation function $N^{(k)}$ is a function of (X_1, X_2), we apply the chain rule to obtain

$$\frac{\partial N^{(k)}}{\partial \xi} = \frac{\partial N^{(k)}}{\partial X_1} \cdot \frac{\partial X_1}{\partial \xi} + \frac{\partial N^{(k)}}{\partial X_2} \cdot \frac{\partial X_2}{\partial \xi} \tag{17a}$$

$$\frac{\partial N^{(k)}}{\partial \eta} = \frac{\partial N^{(k)}}{\partial X_1} \cdot \frac{\partial X_1}{\partial \eta} + \frac{\partial N^{(k)}}{\partial X_2} \cdot \frac{\partial X_2}{\partial \eta} \tag{17b}$$

The corresponding matrix notation is given as

$$
\begin{Bmatrix} \dfrac{\partial N^{(k)}}{\partial \xi} \\ \dfrac{\partial N^{(k)}}{\partial \eta} \end{Bmatrix} = \begin{bmatrix} \dfrac{\partial X_1}{\partial \xi} & \dfrac{\partial X_2}{\partial \xi} \\ \dfrac{\partial X_1}{\partial \eta} & \dfrac{\partial X_2}{\partial \eta} \end{bmatrix} \begin{Bmatrix} \dfrac{\partial N^{(k)}}{\partial X_1} \\ \dfrac{\partial N^{(k)}}{\partial X_2} \end{Bmatrix} \tag{18}
$$

When the above formula is compared with formula (15), we can identify the following relationship:

$$
\begin{bmatrix} \dfrac{\partial \xi}{\partial X_1} & \dfrac{\partial \eta}{\partial X_1} \\ \dfrac{\partial \xi}{\partial X_2} & \dfrac{\partial \eta}{\partial X_2} \end{bmatrix} = \begin{bmatrix} \dfrac{\partial X_1}{\partial \xi} & \dfrac{\partial X_2}{\partial \xi} \\ \dfrac{\partial X_1}{\partial \eta} & \dfrac{\partial X_2}{\partial \eta} \end{bmatrix}^{-1} \tag{19}
$$

Finally, by substituting formula (6) into to the right side of the above equation, we obtain:

$$
\begin{bmatrix} \dfrac{\partial X_1}{\partial \xi} & \dfrac{\partial X_2}{\partial \eta} \\ \dfrac{\partial X_1}{\partial \xi} & \dfrac{\partial X_2}{\partial \eta} \end{bmatrix} = \begin{bmatrix} \dfrac{\partial N^{(k)}}{\partial \xi} X_1^{(k)} & \dfrac{\partial N^{(k)}}{\partial \xi} X_2^{(k)} \\ \dfrac{\partial N^{(k)}}{\partial \eta} X_1^{(k)} & \dfrac{\partial N^{(k)}}{\partial \eta} X_2^{(k)} \end{bmatrix} \tag{20}
$$

As a result, the matrix in the right side of formula (15) can be calculated from formula (19). Thus, the derivative of interpolation function $N^{(k)}$ with respect to X_1 or X_2 can easily be calculated.

(3) Examples of strain field (stretch) in actual tests

Figures 16, 17 and 18 show the distributions of strain fields obtained from the image processing in a uniaxial tension test for material A at the loading speed of 2mm/sec, the one in a strip-biaxial tension test for material D at 2mm/sec, and the one in a equi-biaxial test for material D at 20mm/sec. Figure 16 for the uniaxial tension test and Fig. 17 for the strip-biaxial tension test show that when elongated in the horizontal direction, the material is contracted in the vertical direction as the loading increases. This is because the volume of the material remain constant even though it is deformed.

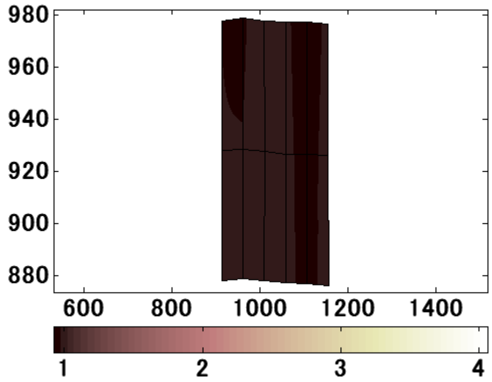

(a) Before deformation

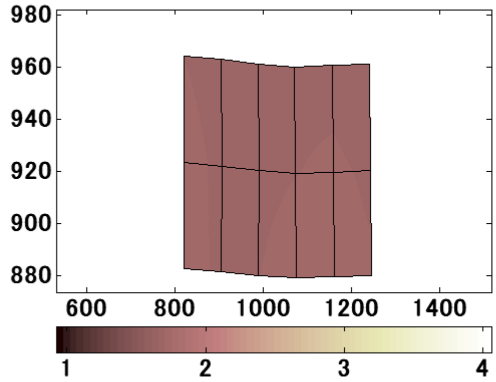

(b) At stretch 1.5

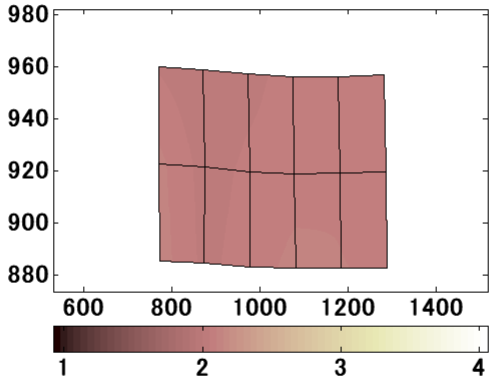

(c) At stretch 2

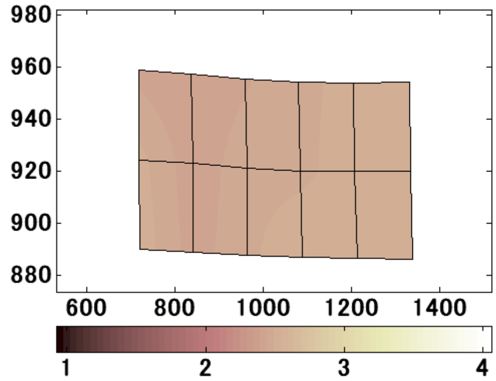

(d) At stretch 2.5

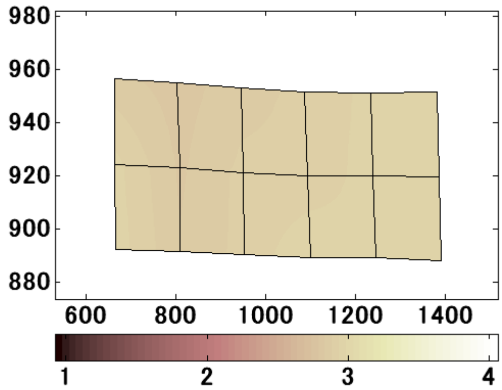

(e) At stretch 3

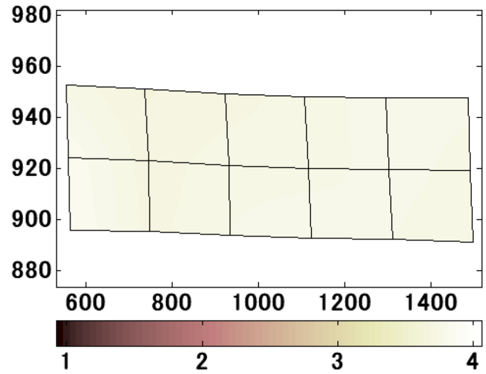

(f) At stretch 3.5

Fig. 16 Strain field obtained from the image processing for uniaxial tension tests on material A at loading speed 2 mm/sec

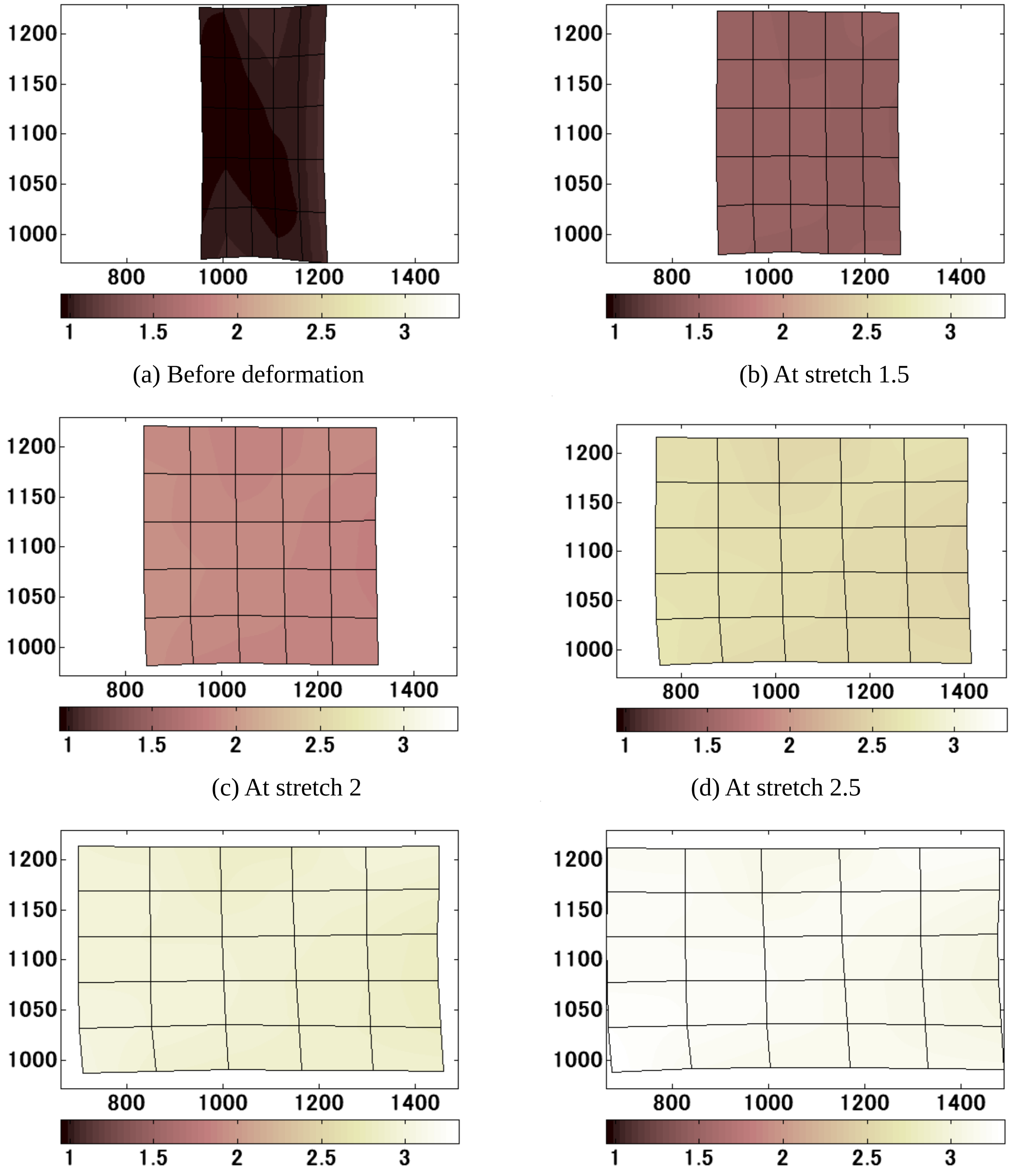

(a) Before deformation

(b) At stretch 1.5

(c) At stretch 2

(d) At stretch 2.5

(e) At stretch 3

(f) At stretch 3.5

Fig. 17 Strain field obtained from the image processing for strip-biaxial tension tests on material D at loading speed 2 mm/sec

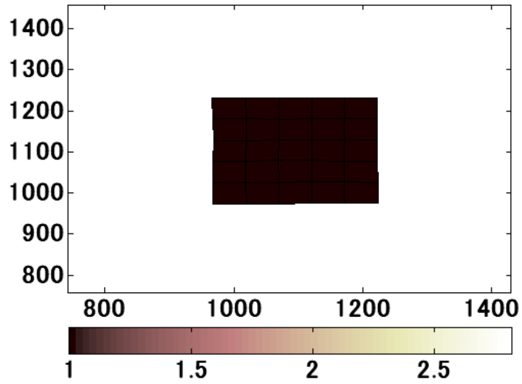

(a) Before deformation

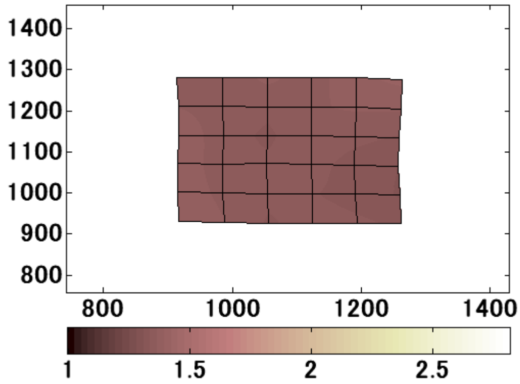

(b) At stretch 1.4

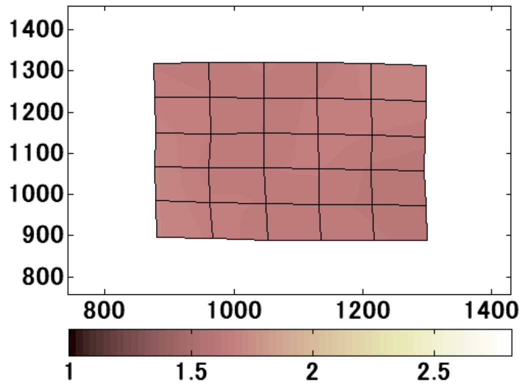

(c) At stretch 1.8

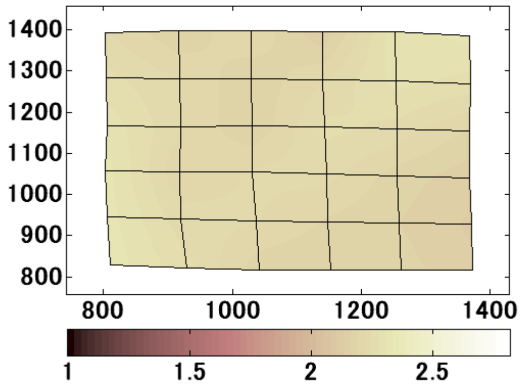

(d) At stretch 2.2

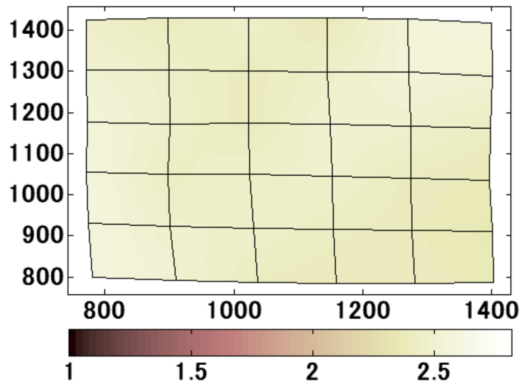

(e) At stretch 2.6

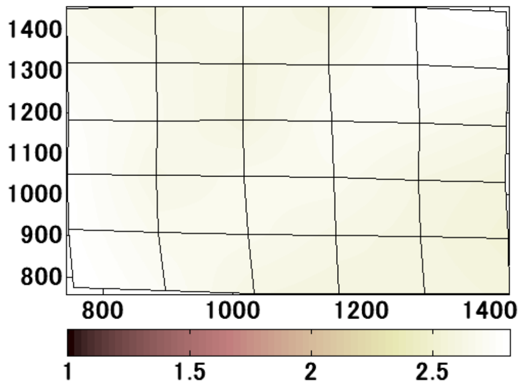

(f) At stretch 3

Fig. 18 Strain field obtained from the image processing for biaxial tension tests on material D at loading speed 20 mm/sec

6 Conclusion

In this report, we firstly presented the outline of the biaxial loading device and discuss the correction of input data to the device. Secondly, we explained the outline of the specimen and the testing method employed in this working group. Finally, by interpolating the displacement values from those of the center point of white markers, we calculated a strain field.